arXiv:0706.2942v1 [astro-ph] 20 Jun 2007

Astrometric effects of solar-like magnetic activity in late-type stars and their relevance for the detection of extrasolar planets

A. F. Lanza [a,*], C. De Martino [a,b], M. Rodonò [a,b,1]

[a] *INAF-Osservatorio Astrofisico di Catania,*

[b] *Dipartimento di Fisica e Astronomia, Università degli Studi di Catania, Via S. Sofia, 78, 95123 Catania, Italy*

Abstract

Using a simple model based on the characteristics of sunspots and faculae in solar active regions, the effects of surface brightness inhomogeneities on the position of the photocentre of the disk of a solar-like, magnetically active star, are studied. A general law is introduced, giving the maximum amplitude of the photocentre excursion produced by a distribution of active regions with a given surface filling factor. The consequences for the detection of extrasolar planets by means of the astrometric method are investigated with some applications to forthcoming space missions, such as GAIA and SIM, as well as to ground-based interferometric measurements. Spurious detections of extrasolar planets can indeed be caused by activity-induced photocentre oscillations, requiring a simultaneous monitoring of the optical flux and a determination of the rotation period and of the level of activity of the target stars for an appropriate discrimination.

Key words: astrometry, stars: activity, planetary systems, stars: spots
PACS: 95.10.Jk, 97.10.Jb, 97.10.Qh, 97.82.Fs

1 Introduction

The distribution of brightness over the solar photosphere is not uniform, due to the presence of dark sunspots and bright faculae in active regions and to

* Corresponding author
Email address: nuccio.lanza@oact.inaf.it (A. F. Lanza).

[1] Deceased

the granular convection and bright network elements, associated with slender flux tubes located in the intergranular lanes. The baricentre of the brightness distribution over the solar disk, i.e., the photocentre of the Sun, is affected by the brightness inhomogeneities having the largest scales, that is by sunspots and faculae, because the averaged effect of the granulation and the network elements is negligible, thanks to their almost uniform distribution on spatial scales comparable with the solar radius. The rotation of the Sun and the evolution of the active regions make the perturbation of the position of the photocentre a function of the time.

Sunspots and faculae are manifestations of the magnetic field, amplified and modulated by the solar dynamo, and are present also on the photospheres of late-type stars hosting hydromagnetic dynamos in their convective envelopes. Therefore, the brightness inhomogeneities observed in the Sun are also present on late-type stars during their main-sequence lifetime and are most prominent in young, rapidly rotating stars, given their more powerful dynamo action (e.g. Lanza & Rodonò, 1999).

The perturbation of the position of the photocentre of late-type stars due to their magnetic activity should be considered in some detail, in view of the forthcoming space missions GAIA [2] and SIM [3]. They will obtain astrometric measurements of the position of late-type stars with $V \leq 10 - 12$ with an accuracy between 1 and 10 μas (micro arc-seconds); see, e.g., Shao et al. (2007). Moreover, ground-based interferometric instruments, such as PRIMA at VLTI [4], will also reach an accuracy of ~ 10 μas in the determination of the photocentre position. The feasibility of such a ground-based high-precision differential astrometry has been recently demonstrated by the PHASES (Palomar High-precision Astrometric Search for Planets) program (see Muterspaugh et al., 2006).

In the present paper, a simple model for computing the astrometric effects of cool spots and bright solar-like faculae in a late-type star is introduced, and applied to derive the maximum expected amplitude of variation of the photocentre position as a function of the active region filling factor. Since the perturbation is cyclically modulated by the stellar rotation, it can be a source of spurious detections of close-by planetary companions by means of the astrometric technique. We present some cases leading to possible confusion and propose methods to discriminate the effects of a planet from those due to stellar activity.

[2] See http://www.rssd.esa.int/Gaia
[3] See http://sim.jpl.nasa.gov/
[4] See http://www.eso.org/projects/vlti/instru/prima/index_prima.html

2 The model

Let us consider a Cartesian reference frame with the $\hat{x}$-$\hat{y}$ plane in the plane of the sky, that is the origin O at the unperturbed photocentre of the star, the $\hat{x}$-axis along the declination direction pointing to the North pole, the $\hat{y}$-axis along the direction of the increasing right ascension and the $\hat{z}$-axis pointing toward the observer. The position $(x_{\rm p}, y_{\rm p})$ of the photocentre at a given time t depends on the distribution of the brightness on the surface of the apparent disk of the star at the isophotal wavelength λ of the observations, and is given by:

$$\begin{aligned} x_{\rm p} &= \frac{\int\limits_D I(\lambda,x,y)x dS}{\int\limits_D I(\lambda,x,y) dS}, \\ y_{\rm p} &= \frac{\int\limits_D I(\lambda,x,y)y dS}{\int\limits_D I(\lambda,x,y) dS}, \end{aligned} \tag{1}$$

where I is the specific intensity at wavelength λ at the given position (x, y) on the stellar disk, and the integration is extended over the apparent stellar disk D. Equations (1) define the photocentre as the baricentre of the flux distribution emerging from the stellar disk. For an unperturbed star, such a distribution is symmetric around the disk centre and the photocentre coincides with the projection of the baricentre of the star on the plane of the sky.

In order to describe the distribution of the surface brightness when there are photospheric inhomogeneities, it is more convenient to adopt a spherical reference frame rotating with the star. Specifically, a spherical reference frame is considered with the origin at the baricentre $\rm O_B$ of the star and the $\hat{z_0}$-axis directed along its rotation axis, rotating with the stellar angular velocity Ω with respect to an inertial reference frame. We can express the position of a generic point on the stellar surface by means of its Cartesian co-ordinates in that frame:

$$\begin{cases} x_0 = \mathcal{R}\sin\theta\cos l, \\ y_0 = \mathcal{R}\sin\theta\sin l, \\ z_0 = \mathcal{R}\cos\theta, \end{cases} \tag{2}$$

where $\mathcal{R}$ is the radius of the star, assumed to be spherically symmetric, and θ and l are the colatitude and the longitude of the point on the stellar surface, respectively. The transformation from the latter reference frame to the reference frame of the stellar disk can be achieved by means of three successive Eulerian rotations. In order to define them, let us consider that the stellar equatorial plane intersects the plane of the sky along a line of nodes that makes an angle Φ with respect to the direction of the $\hat{x}$-axis on the plane of the sky. The first rotation by an angle $\omega = -\Omega(t - t_0)$ around the $\hat{z}_0$-axis makes the fundamental stellar meridian coincide with its position at the time t_0 when it crosses the line of nodes. The second rotation by the inclination i of the stellar rotation axis, around the line of nodes, makes the $\hat{z}_0$-axis coincide with the $\hat{z}$ axis. Finally, a rotation by an angle Φ, around the $\hat{z}$ axis, reports the reference frame into that of the plane of the sky.

In matrix form, we can write the co-ordinate transformation as follows:

$$\begin{bmatrix} x \\ y \\ z \end{bmatrix} = \tilde{A} \begin{bmatrix} x_0 \\ y_0 \\ z_0 \end{bmatrix}, \tag{3}$$

where $\tilde{A}$ is the transformation matrix that is given by:

$$\tilde{A} = \begin{pmatrix} \cos\Phi & \sin\Phi & 0 \\ -\sin\Phi & \cos\Phi & 0 \\ 0 & 0 & 1 \end{pmatrix} \begin{pmatrix} 1 & 0 & 0 \\ 0 & \cos i & \sin i \\ 0 & -\sin i & \cos i \end{pmatrix} \begin{pmatrix} \cos\omega & \sin\omega & 0 \\ -\sin\omega & \cos\omega & 0 \\ 0 & 0 & 1 \end{pmatrix}, \tag{4}$$

where the individual factor matrixes express the three rotations as specified above, respectively. Note that the angle ω is a linear function of the time, whereas i and Φ are constant.

We subdivide the photosphere of the star into $1^\circ \times 1^\circ$ elements, each of which is identified by the longitude l and colatitude θ of its central point. The status of the photosphere in each element can be either unperturbed, spotted, or of facular type. The specific intensity of the unperturbed photosphere is assumed to be given by a linear limb-darkening law:

$$I(\lambda, \mu) = I_0(\lambda)(1 - u_\lambda + u_\lambda \mu), \tag{5}$$

where $I_0(\lambda)$ is the specific intensity at the centre of the disk, u_λ the linear limb-darkening coefficient at the isophotal wavelength λ, and $\mu \equiv \cos\psi$, where ψ

is the angle between the normal to the given surface element and the line of sight. It is given by:

$$\mu = \sin\theta \sin i \cos\left[l + \Omega(t - t_0)\right] + \cos\theta \cos i. \tag{6}$$

The specific intensity of the spotted photosphere is given by: $I_{\rm s}(\lambda,\mu) = c_{\rm s}(\lambda) I(\lambda,\mu)$, where the spot contrast $c_{\rm s} < 1$ is a function of the wavelength λ and is assumed to be independent of μ (cf. Lanza et al., 2004). The specific intensity of the facular photosphere is assumed to be equal to that of the unperturbed photosphere at the disk centre, while its contrast increases linearly toward the limb, i.e., $I_{\rm f}(\lambda,\mu) = I(\lambda,\mu)[1 + c_{\rm f}(\lambda)(1-\mu)]$, with the constrast coefficient $c_{\rm f}$ being a function of the wavelength (see Lanza et al., 2004, for details). The value of the flux coming from the i-th surface element at the wavelength λ and the time t_k is given by:

$$\Delta F_i(\lambda, t_k) = \begin{cases} I[\lambda, \mu(t_k)] \Delta A_i \mu(t_k) g[\mu(t_k)] & \text{for the unperturbed photosphere,} \\ I_{\rm s}[\lambda, \mu(t_k)] \Delta A_i \mu(t_k) g[\mu(t_k)] & \text{for the spotted photosphere,} \\ I_{\rm f}[\lambda, \mu(t_k)] \Delta A_i \mu(t_k) g[\mu(t_k)] & \text{for the facular photosphere,} \end{cases} \tag{7}$$

where g is the visibility function of the surface element, i.e., $g(\mu) = 1$ for $\mu \geq 0$, $g(\mu) = 0$ for $\mu < 0$. The total flux from the stellar disk at time t_k is: $F(\lambda, t_k) = \sum_i \Delta F_i(\lambda, t_k)$. The co-ordinates of the photocentre on the plane of the sky at time t_k are given by:

$$\begin{aligned} x_{\rm p} &= \frac{\sum\limits_i x_i(t_k) \Delta F_i(\lambda, t_k)}{\sum\limits_i \Delta F_i(\lambda, t_k)}, \\ y_{\rm p} &= \frac{\sum\limits_i y_i(t_k) \Delta F_i(\lambda, t_k)}{\sum\limits_i \Delta F_i(\lambda, t_k)}, \end{aligned} \tag{8}$$

where the co-ordinates x_i and y_i depend on the spherical co-ordinates l_i, θ_i of the i-th surface element and the geometrical parameters of the star through Eqs. (2) and (3). From Eq. (8), we see that $x_{\rm p}$ and $y_{\rm p}$ depend on the isophotal wavelength of the observations. It can be assumed to be fixed for a given astrometric instrument, hence we shall not consider explicitly that dependence.

Other effects affecting the position of the photocentre, e.g., the oscillations due to a planet or a planetary system (e.g. Sozzetti et al., 2003), or the proper motion of the star, can be linearly added up to the effects of the surface brightness inhomogeneities computed with the scheme introduced above.

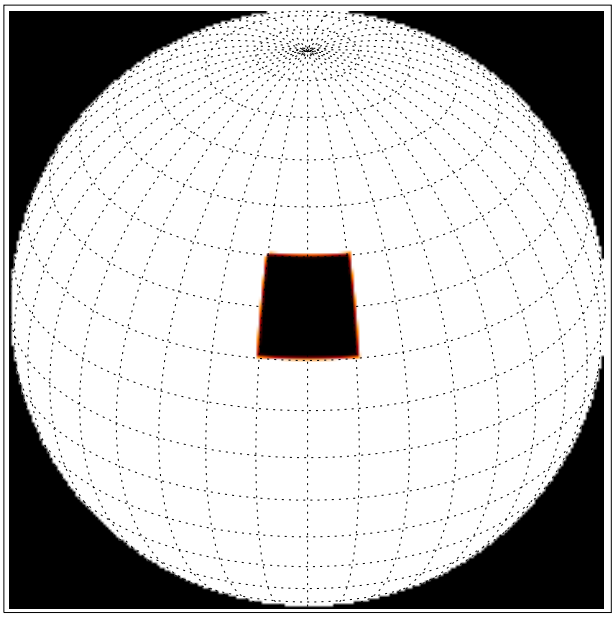


Fig. 1. The disk of our model star with the spotted region of $20^\circ \times 20^\circ$ as seen by the observer at the rotation phase when the active region transits across the central disk meridian. The inclination of the stellar rotation axis with respect to the line of sight is 60°, thus the centre of the active region passes through the centre of the star disk.

3 Results

We have applied the model described in Sect. 2 to compute the apparent motion of the photocentre of a star with a single active region on its surface, containing only cool spots and having a longitudinal extension of 20° between latitudes 20° and 40° in the Northern hemisphere. The active region has an area of 0.83% of the whole stellar surface, i.e., about $\sim 8 - 10$ times larger than the area of the largest sunspot groups at the maximum of the eleven-year cycle. However, we believe this is more appropriate for late-type stars that are slightly more active than the Sun (see Sect. 4. For the sake of simplicity, our model spotted region is assumed to be uniform in contrast and squared in shape (see Fig. 1). However, as we shall see below, the maximum photocentre excursion depends primarily on the total area of the active region with its shape playing a secondary role. The limb-darkening coefficient of the unperturbed photosphere is assumed to be $u_\lambda = 0.65$ at the given isophotal wavelength and the spot contrast $c_\mathrm{s} = 0.33$, which is appropriate to describe the bolometric flux perturbation in the case of sunspots, corresponding to an effective temperature of the spotted photosphere of ~ 4400 K, i.e., ~ 1400 K below that of the unperturbed photosphere, which accounts, on average, for the combined effects of umbrae and penumbrae (e.g., Chapman et al., 1994). In Fig. 2, we plot the position of the photocentre versus the rotational phase

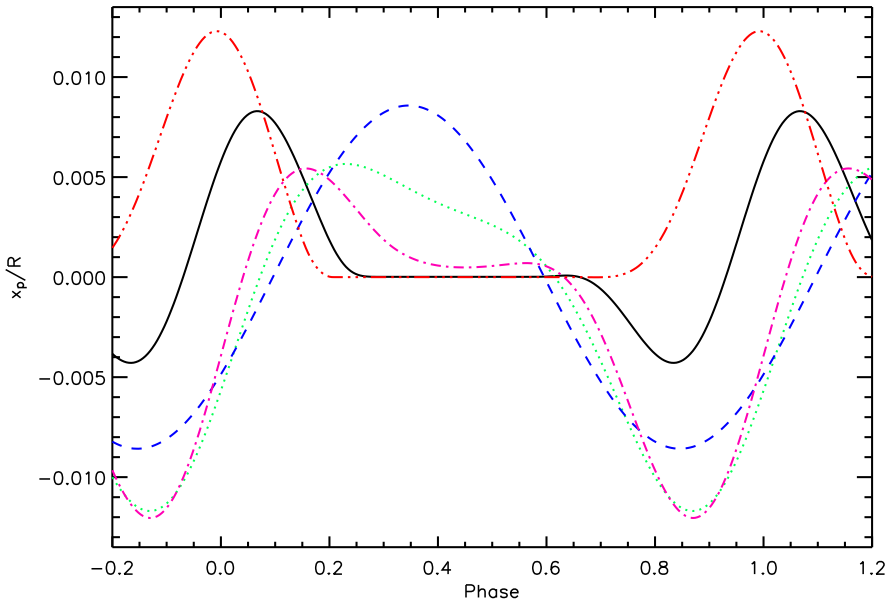


Fig. 2. The relative abscissa $x_{\rm p}$ of the photocentre of our model star on the plane of the sky versus the rotational phase. The unit of measure of the abscissa is the apparent radius R of the stellar disk. Different linestyles and colors refer to different values of the inclination i of the rotation axis: dashed blue – $i = 0°$ (i.e., pole-on view); dotted green – $i = 15°$; dot-dashed pink – $i = 30°$; solid black – $i = 60°$; and three-dot-dashed red – $i = 90°$ (i.e., equator-on view).

for different values of the inclination i of the stellar rotation axis along the line of sight. The photocentre excursion is measured in unit of the apparent radius of the stellar disk R along the direction of the $\hat{x}$-axis, adopting a position angle $\Phi = 30°$ in our calculations. The motion along the $\hat{y}$-axis is similar, but shifted in phase by an amount that depends on the co-ordinates of the active region and the stellar parameters i and Φ. The active region is assumed to be stable, so that stellar rotation is the only effect responsible for the motion of the photocentre. The variations of the relative flux corresponding to the simulations shown in Fig. 2 are plotted in Fig. 3. When the inclination is lower than 20°, the active region is always in view and produces a continuous modulation of the position of the photocentre and of the flux that depends on the variation of its position on the stellar disk and its projected area. For a pole-on view, the projected area is constant and the variation of the photocentre abscissa is purely sinusoidal, whereas the flux stays constant. When the inclination increases, the modulation of the photocentre abscissa is no longer sinusoidal. When $i \geq 50°$, there are intervals of phase during which the photocentre is unperturbed, i.e., when the active region transits on the invisible hemisphere of the star. Considering the case with $i = 60°$, we note that, when the active region first appears on the rising part of the disk, it produces a negative shift of the photocentre abscissa because the baricentre of the flux distribution falls in the opposite half of the disk. Then the shift

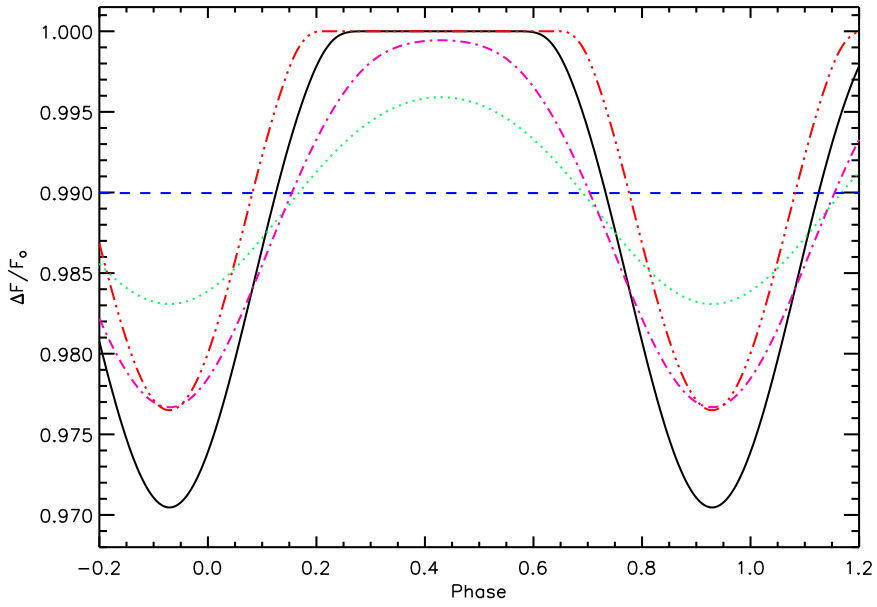


Fig. 3. The relative variation of the stellar flux as a function of the rotational phase for the cases simulated in Fig. 2. The unit of flux F_0 corresponds to the unperturbed flux of the star. Different linestyles and color indicate different values of the inclination, as in Fig. 2.

reverses its sign, when the active region is carried by stellar rotation on the other half of the disk, and eventually it becomes zero when the active region comes out of view. For $i \neq 90°$, the duration of the active region transit across the disk depends on its average latitude and the inclination. Moreover, the sign and the value of the photocentre excursion depend also on the position angle of the projection of the stellar rotation axis on the plane of the sky, as measured by the angle Φ. The combination of these different factors explains the different shapes and amplitudes of the curves plotted in Fig. 2.

The flux variation produced by the active region increases with increasing inclination and reaches its maximum value when the active region transits through the centre of the stellar disk, i.e., for $i = 60°$, because in that case its projected area reaches its maximum value. Note that the excursion of the photocentre and the flux variations are correlated for $i > 0°$, as shown in Fig. 4.

When only a single active region is present on the stellar disk, the excursion of the photocentre reaches its maximum value for a given value of the total active region area. As a matter of fact, if the same total area is subdivided into two or more active regions, the excursion generally decreases because the simultaneous presence of more than one brightness inhomogeneity leads to a reduction of their combined effects. Therefore, we have investigated the variation of the maximum photocentre excursion $\Delta r \equiv \max\left\{\sqrt{(\Delta x_{\rm p})^2 + (\Delta y_{\rm p})^2}\right\}$

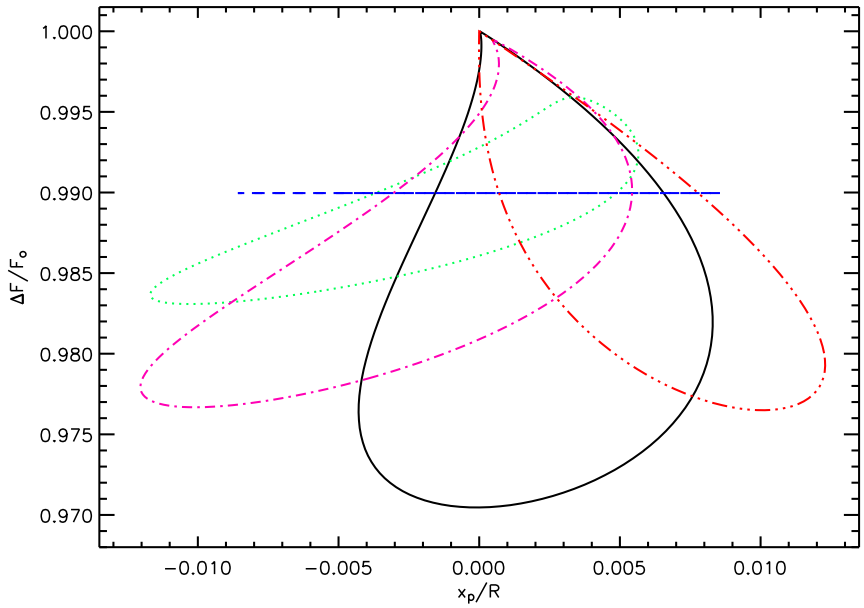


Fig. 4. The relative flux variation versus the photocentre abscissa for the cases simulated in Fig. 2. Different linestyles and colors indicate different values of the inclination, as in Fig. 2. Note the correlation between the photocentre motion and the flux variation, and the degenerate case corresponding to $i = 0°$.

as a function of the filling factor f for a single active region by means of our model (see Fig. 5). The stellar inclination is assumed fixed at $i = 60°$, that is the most probable value for a random orientation of the stellar rotation axis. The average latitude of the active region is 30° to maximize its effect on the position of the photocentre. In those simulations, we consider also the effect of a facular component that surrounds the dark spot. The area of the facular component is assumed to be ten times that of the cool spots, as suggested by solar observations and modelling of the solar irradiance variations (see, e.g., Lanza et al., 2003, 2007, and references therein). The spot constrast is assumed to be $c_s = 0.33$, while the facular contrast is $c_f = 0.15$ (see, e.g., Lanza et al., 2007). Note that the effect of the faculae is small, in spite of their relative area being ten times that of cool spots. This is due to the fact that their effect is significant only close to the limb, because their contrast is negligible close to the centre of the disk. Moreover, the projection effect disfavours the facular contribution, because their projected area becomes small close to the limb. The situation changes if we consider hot spots instead of solar-like faculae, that is bright regions the constrast of which is significant also close to the disk centre, as is sometimes observed in the case of very active stars (cf., e.g., the case of the active component of the RS CVn binary system HR 1099 reported by Vogt et al., 1999). However, since we are here mainly interested in solar-like stars, we shall not consider further this possibility.

The variation of the amplitude of the rotational modulation of the stellar flux

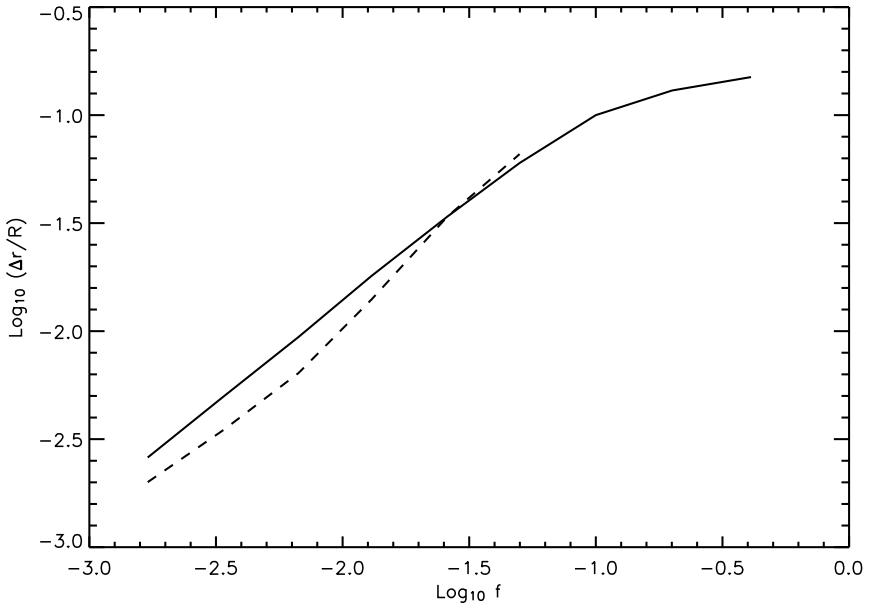


Fig. 5. The relative excursion $\Delta r/R$ of the photocentre versus the spot filling factor f in the case of a single active region for an inclination of the stellar rotation axis of $i = 60°$. The solid line refers to the case of an active region consisting only of dark spots, whereas the dashed line refers to an active region with dark spots surrounded by solar-like faculae (see the text).

versus the filling factor is plotted in Fig. 6. The correlations shown in Figs. 5 and 6 can be well approximated by power laws up to a value of the filling factor $f \simeq 0.1$, beyond which they deviate from such a simple dependence because the amplitude of the variation saturates when a large fraction of the stellar disk is covered with active regions. Applying a linear best fit to the plots in Figs. 5 and 6, we find the following regression expressions, valid for $f \leq 0.1$, with a correlation coefficient $\rho > 0.99$:

$$\log_{10} \frac{\Delta r}{R} = (-0.055 \pm 0.031) + (0.907 \pm 0.016) \log_{10} f (\text{dark spots only}),$$
$$\log_{10} \frac{\Delta r}{R} = (0.176 \pm 0.089) + (1.059 \pm 0.042) \log_{10} f (\text{spots \& faculae}), \quad (9)$$

and

$$\log_{10} \frac{\Delta F}{F_0} = (0.343 \pm 0.014) + (0.917 \pm 0.007) \log_{10} f (\text{dark spots only}),$$
$$\log_{10} \frac{\Delta F}{F_0} = (0.296 \pm 0.034) + (0.902 \pm 0.017) \log_{10} f (\text{spots \& faculae}), \quad (10)$$

where the reported uncertainties correspond to one standard deviation. The first of Eqs. (9) confirms the results previously obtained by Hatzes (2002) in

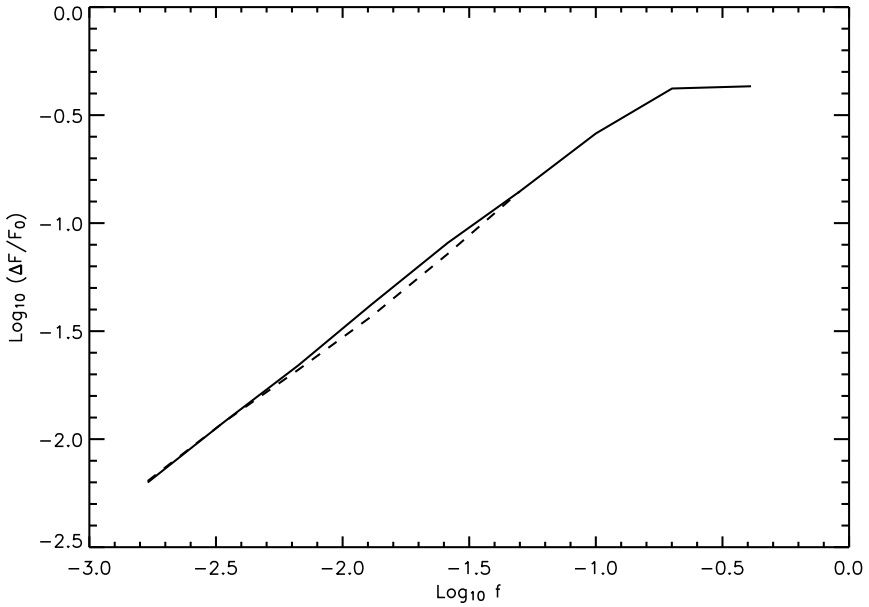


Fig. 6. The relative flux variation $\Delta F/F_0$ versus the spot filling factor f in the case of a single active region for an inclination of the stellar rotation axis of $i = 60°$. The solid line refers to the case of an active region consisting only of dark spots, whereas the dashed line refers to an active region with dark spots surrounded by solar-like faculae (see the text).

the case of an active region consisting of dark spots only. Muterspaugh et al. (2006) also estimated upper limits for the astrometric effect of dark spots assuming a simplified model with a fixed projected spot geometry and neglecting limb-darkening effects. Their model confirms the almost linear correlation between the variation of the stellar flux and the photocentre excursion that can be deduced combining together Eqs. (9) and (10). However, they predict an astrometric effect about 60% larger than ours for a given photometric amplitude, essentially because of the neglection of the foreshortening and limb-darkening effects.

Note that the simultaneous presence of spots and faculae decreases the photocentre excursion in our model and makes the regression more steep, especially for $f \leq 0.03$. This is due to the opposite effects of bright and dark regions spatially associated on the stellar disk. For a filling factor larger than 0.03, the effect of the faculae becomes negligible because of their low contrast close to the centre of the disk that leads to a saturation of their contribution.

Equations (9) and (10) can be used to estimate the maximum relative photocentre excursion and flux variation, respectively, expected for a given spot coverage in a solar-like star. This is useful to evaluate the possibility that stellar activity may account for an observed shift of the photocentre in a late-type star.

Table 1
The seven stars with an apparent radius R larger than 1000 μas and spectral type later than F5, listed in order of decreasing R.

HIP	Name	Sp	V (mag)	$\mathcal{R}$ ($\mathcal{R}_\odot$)	D (pc)	R (μas)
71683	α Cen A	G2V	-0.01	0.91	1.347 ± 0.003	3146
71681	α Cen B	K1V	1.35	0.76	1.347 ± 0.003	2629
37279	α CMi	F5IV-V	0.40	1.32	3.497 ± 0.011	1761
87937	Barnard's star	M5V	9,54	0.57	1.821 ± 0.005	1468
8102	τ Cet	G8V	3.49	0.90	3.647 ± 0.011	1153
16537	ϵ Eri	K2V	3.72	0.76	3.218 ± 0.009	1101
54035	Gl 411	M2Ve	7.49	0.57	2.548 ± 0.006	1041

4 Application to nearby stars and consequences for planetary detections

The effects of stellar magnetic activity on the position of the photocentre can be principally observed in nearby solar-like stars, because the maximum excursion cannot exceed the apparent stellar radius. Considering the one hundred nearest stars listed in the catalogue of Cox (2000), those with spectral type between F0V and M5V and apparent magnitude $V \leq 11$ have been selected for a quantitative study. They are within ~ 7.6 pc from the Sun. Their radii have been estimated from their $B-V$ color indexes according to Gray (1992), whereas their distances are taken from the Hipparcos catalogue. Seven stars turn out to have an apparent radius R larger than 1000 μas and are listed in Table 1 where the columns from the left to the right give the number in the Hipparcos catalogue, the name, the spectral type, the apparent visual magnitude, the radius, the distance (with its standard deviation), and the apparent radius of each star, respectively. Moreover, 13 stars turn out to have an apparent radius between 700 and 1000 μas, while 46 have an apparent radius $350 \leq R \leq 700$ μas. The results obtained in Sect. 3 show that for a filling factor of 0.2%, corresponding to the Sun at the maximum of the eleven-year cycle, excursions as large as ~ 8 μas can be expected for α Cen A in the case of an active region consisting only of cool spots. In the case of an active region

containing also solar-like faculae, those values are reduced by a factor of ~ 1.4 because the faculae tend to decrease the effect of the spots at such a low value of the filling factor. A solar value of the filling factor is likely to be appropriate for α Cen A because the star appears to have a level of activity comparable or slightly lower than the Sun, with a rotation period of about 29 days (see, e.g., Pagano et al., 2004). Note that the above estimates refer to the case of a single active region, thus the excursion can be reduced if a few active regions are simultaneously present on the stellar disk. In any case, those amplitudes will be easily detectable by astrometric space-borne experiments like GAIA and SIM, and could be within the reach of ground-based interferometers, such as PRIMA. Note that a periodic signal can be detected with high confidence in a sufficiently long time series, even if the errors on the single measurements are larger than its amplitude (see, e.g., Horne & Baliunas, 1986). In the Sun, the average lifetime of the sunspot groups dominating the flux modulation is $\sim$ 14 days (cf., e.g., Lanza et al., 2003, 2007), but they have a remarkable tendency to form in sequence within activity complexes, the lifetime of which is $\sim 3-6$ months (e.g., Gaizauskas et al., 1983).

Therefore, if an activity complex on α Cen A is stable for a time interval longer than the rotation period, it can produce a cyclic modulation of the position of the photocentre with a semi-amplitude up to ~ 8 μas and a period of 29 days that can be erroneously attributed to the reflex motion induced by a planet of $\lesssim 20$ Earth masses on an orbit of semi-major axis of ~ 0.18 AU, assuming that the star has the same mass of the Sun. Such a spurious detection is difficult to disprove by correlating the photocentre motion with the variation of the stellar optical flux, as measured by ground-based photometry, because the expected amplitude of variation is only ~ 0.006 mag (cf. Fig. 6 and Eq. 10).

On the average, the level of activity is expected to be higher than solar for the stars of spectral types later than the Sun listed in Table 1, because their convection zones are deeper and their rotation periods are comparable or shorter than the solar one (cf., e.g., Weiss, 1994). The expectation is confirmed in the case of ϵ Eri, for which spot modelling of MOST photometry indicates a filling factor of at least 0.7% (Croll et al., 2006). This implies a maximum excursion of ~ 9 μas for the photocentre position with the rotation period of the star, i.e., ~ 11.3 days. Moreover, the observations indicate that the signal would maintain its coherence for several rotations because the timescale of spot evolution is longer than 35 days. The observed amplitude of the optical flux variation of ϵ Eri is only ~ 0.014 mag, that is at the detection limit of ground-based photometry.

It is interesting to note that ϵ Eri has a planetary companion on a wide orbit with a period of 6.8 years (e.g., Benedict et al., 2006). The astrometric orbit has a semi-major axis of 1.88 ± 0.20 mas (milli arcseconds), that is much larger than the astrometric noise expected to be produced by stellar activity. The

inclination of the planetary orbit is $i_{\rm p} = 30^\circ.1 \pm 3^\circ.8$. Assuming that the stellar spin and the orbital angular momentum are aligned, we can adopt the same inclination for the stellar rotation axis. This implies that all the active regions located at latitudes higher than 30° are circumpolar and produce a continuous modulation of the photocentre position with the stellar rotation period. They can give rise to a spurious detection of further planetary companions around ϵ Eri. Specifically, assuming a stellar mass of 0.83 $M_\odot$, a photocentre oscillation with a period of 11.3 days and an amplitude of 9 μas can be attributed to a planet of ~ 0.3 Jupiter masses on an orbit of semi-major axis 9.26×10^{-2} AU.

Late-type stars with rotation periods of a few days have spot filling factors of the order of $f \sim 0.05 - 0.1$ (cf., e. g., Messina et al., 2003). They can produce astrometric signatures with amplitudes up to 0.1 stellar radii, i.e., up to ~ 30 μas in the group of 66 nearby stars considered above. If we extend our sample to the solar-type stars within 60 pc from the Sun, at least 13,000 objects brighter than $V = 13$ are expected to be observable by GAIA with an astrometric precision between 5 and 10 μas (Sozzetti et al., 2001). The apparent radius of the Sun at a distance of 60 pc is 78 μas, implying that the most active stars in the sample (at least 2%−3%) should display measurable astrometric effects at the level of $5 - 10$ μas. The cyclic modulation of the signal with the rotation period is much shorter than the typical timescales of starspot evolution, that range typically between ~ 5 and ~ 16 months (Messina & Guinan, 2003). As a consequence, the astrometric modulation is quasi-stable, increasing the probability of spurious planetary detections. Of course, the correlation of the astrometric signal with the photometric variation can be used to discriminate between activity-induced and planetary-induced photocentre motions. Such stars would have relative flux variations of the order of 0.1 mag, that is about $30 - 100$ times larger than the photometric precision of GAIA. However, the unknown value of the inclination of the stellar rotation axis leaves an ambiguity in those cases in which no flux variation can be detected.

5 Discussion and conclusions

We have pointed out the importance of taking into account the astrometric effects of surface brightness inhomogeneities in future astrometric search for extrasolar planets, in particular of planets with an orbital period of a few days or a few tens of days around late-type stars. The simultaneous measurement of stellar wide-band fluxes offers a powerful tool to discriminate activity-induced effects from the reflex motion of the photocentre induced by an orbiting body. However, the cases of nearby stars, such as α Cen or ϵ Eri, or of rotators observed almost pole-on require some additional methods to investigate the possible effects of magnetic activity. The fraction of stars having an inclination

lower than, say, 20° is 6.0%, which implies that at least a few tens of ambiguous cases should be expected in the GAIA sample of stars within 60 pc.

A further method of discrimination in those cases comes from the fact that the activity-induced motion has the same period of the rotation of the star. If the inclination is not too low, it can be measured from the modulation of the chromospheric Ca II H & K or Ca infrared triplet fluxes, even for stars with an activity level as low as the Sun (e.g., Baliunas et al., 1995; Andretta et al., 2005), or can be roughly estimated from the spectroscopic $v \sin i$ and an assumed stellar radius. Conversely, when the star is viewed almost pole-on, no rotational modulation is expected, but the level of activity can be estimated from those chromospheric indicators as well as from the stellar X-ray flux.

These considerations indicate the importance of a characterization of the level of activity and the determination of the rotation period for those stars that have been selected as potentially planet-harbouring objects by means of the astrometric method. This is particularly important when the measurement samples consist of widely separated data, as will be the case for GAIA that will observe a given star for about 80 times in five years, on the average. Dedicated simulations, based on the observed positions of solar active regions along an entire activity cycle and the time-sampling law of GAIA, are required to assess the impact of stellar activity on GAIA long-term astrometry for solar-like stars. This will be the subject of a future work. Here we limit ourselves to some general considerations based on solar analogy.

Individual spot groups will grow and decay on timescales of a few weeks, nevertheless the astrometric signal due to photospheric activity may show some phase coherence for timescales comparable with the lifetimes of complexes of activity. In the case of sunspot complexes, those timescales do not exceed $5-6$ solar rotations (Gaizauskas et al., 1983). However, Schröter (1984) reported the persistence of two chromospheric active regions separated by $\sim 180°$ in longitude for time intervals longer than ~ 500 days during periods of moderate or high solar activity. If a similar behaviour characterizes magnetic activity in other solar-like stars, this can give rise to spurious planetary detections given that the astrometric signal produced by two active regions separated by $\sim 180°$ in longitude shows a sinusoidal oscillation with a period half that of stellar rotation.

Stars with a level of activity significantly higher than our Sun often show active longitudes of spot activity lasting for decades (see, e.g., Rodonò et al., 2000, 2001; Lanza et al., 2002; García-Alvarez et al., 2003; Lanza et al., 2006) that can give rise to spurious astrometric detections of bodies orbiting around them. Modelling of the wide-band fluxes of highly active stars indicates that cool spots usually dominate their photometric variations. Moreover, extrapolations

based on solar observations at different levels of activity along the 11-yr cycle, support the conclusion that their active regions are dominated by cool spots with bright faculae playing a secondary role (Foukal, 1998). This implies that their activity-induced astrometric signal can be estimated from the first of equations (9) (or the corresponding plot in Fig. 5 for $f \geq 0.1$).

Acknowledgements

AFL and CDM wish to dedicate this work to Marcello Rodonò, Professor of Astronomy in the University of Catania and Director of the Astrophysical Observatory of Catania, who suddenly passed away during the preparation of the present paper. The authors wish to thank the anonymous Reviewers for their valuable comments. AFL wishes to thank Drs. M. G. Lattanzi and A. Spagna for useful discussions.

Active star research at INAF-Catania Astrophysical Observatory and the Department of Physics and Astronomy of Catania University is funded by MIUR (*Ministero dell'Università e della Ricerca*), and by *Regione Siciliana*, whose financial support is gratefully acknowledged.

This research has made use of the ADS-CDS databases, operated at the CDS, Strasbourg, France.

References

Andretta, V., Busà, I., Gomez, M. T., Terranegra, L. 2005, A&A, 430, 669

Baliunas, S. L., Donahue, R. A., Soon, W. H., Horne, J. H., Frazer, J., et al. 1995, ApJ, 438, 269

Benedict, G. F., McArthur, B. E., Gatewood, G., Nelan, E., Cochran, W. D., et al. 2006, AJ, 132, 2206

Chapman, G. A., Cookson, A. M., Dobias, J. J. 1994, ApJ, 432, 403

Cox, A. N. 2000, Allen's astrophysical quantities, Springer-Verlag, New York

Croll, B., Walker, G. A. H., Kuschnig, R., Matthews, J. M., Rowe, J. F., et al., 2006, ApJ, 648, 607

Foukal, P. 1998, ApJ, 500, 958

Gaizauskas, V., Harvey, K. L., Harvey, J. W., Zwaan, C. 1983, ApJ, 265, 1056

García-Alvarez, D., Foing, B. H., Montes, D., Oliveira, J., Doyle, J. G., et al. 2003, A&A 397, 285

Gray, D. F. 1992, The observations and analysis of stellar photospheres, 2nd Ed., Cambridge Univ. Press, Cambridge

Hatzes, A. P. 2002, Astron. Nach., 323, 392

Horne, J. H., Baliunas, S. L. 1986, ApJ, 302, 757

Lanza, A. F., Bonomo, A. S., Rodonò, M. 2007, A&A 464, 741
Lanza, A. F., Catalano, S., Rodonò, M., Ibanoglu, C., Evren, S., et al. 2002, A&A 386, 583
Lanza, A. F., Piluso, N., Rodonò, M., Messina, S., Cutispoto, G. 2006, A&A 455, 595
Lanza, A. F., Rodonò, M. 1999, in Solar and stellar activity: similarities and differences, C. J. Butler and J. G. Doyle (Eds.), ASP Conf. Ser., 158, p. 121
Lanza, A. F., Rodonò, M., Pagano, I., Barge, P., Llebaria, A. 2003, A&A 403, 1135
Lanza, A. F., Rodonò, M., Pagano I. 2004, A&A, 425, 707
Messina, S., Guinan, E. F. 2003, A&A, 409, 1017
Messina, S., Pizzolato, N., Guinan, E. F., Rodonò, M. 2003, A&A, 410, 671
Muterspaugh, M. W., Lane, B. F., Konacki, M., Burke, B. F., Colavita, M. M., Kulkarni, S. R., Shao, M. 2006, A&A, 446, 723
Pagano, I., Linsky, J. L., Valenti, J., Duncan, D. K. 2004, A&A 415, 331
Rodonò, M., Messina, A. F., Lanza, A. F., Cutispoto, G., Teriaca, L. 2000, A&A 358, 624
Rodonò, M., Cutispoto, G., Lanza, A. F., Messina, S. 2001, Astron. Nach., 322, 333
Shao, M., Marcy, G., Unwin, S., Allen, R., Beichman, C., et al., 2007, arXiv:0704.0952v1
Schröter, e. H. 1984, A&A, 139, 538
Sozzetti A, Casertano, S., Brown, R. A., Lattanzi, M. G. 2003, PASP, 115, 1072
Sozzetti A, Casertano, S., Lattanzi, M. G., Spagna, A. 2001, A&A, 373, L21
Vogt, S. S., Hatzes, A. P., Misch, A. A., Kürster, M. 1999, ApJS, 121, 547
Weiss, N. O. 1994, in Lectures on Solar and Planetary Dynamos, M. R. E. Proctor and A. D. Gilbert (Eds.), Publication of the Newton Institute, Cambridge Univ. Press, Cambridge; p. 59